A Systematic Application of Density Functional Theory to Some Carbon-Containing Molecules and Their Anions

Shawn T. Brown,† Jonathan C. Rienstra-Kiracofe, and Henry F. Schaefer, III*

Center for Computational Quantum Chemistry, University of Georgia, Athens, Georgia 30602

Received: November 9, 1998; In Final Form: February 22, 1999

Eight medium-sized carbon-containing molecules: linear carbon chains C_n ($n = 6-9$), triacetylene (C_6H), tetracyanoethylene (C_6N_4), 1,1,1-trifluoroacetone enolate (CF_3CHCHO), and C_4O have been studied using six different density functional or hybrid Hartree−Fock density functional methods with a double-ζ basis set with polarization and diffuse functions (DZP++). Optimized geometries, harmonic vibrational frequencies, and adiabatic electron affinities were estimated and compared to known experimental values. The harmonic vibrational frequencies showed an overall agreement with experimental fundamentals of approximately 4−6% with one exception, the BHLYP functional. Average absolute errors in electron affinities estimated with the BP86, BLYP, and B3LYP functionals all show agreement of better than 0.2 eV with experiment and provide a viable method of predicting electron affinities for molecules of the same type as studied here.

I. Introduction

Density functional theory (DFT) has been applied to molecular systems with considerable success.[1] The application of the theory to negatively charged molecules has in the recent past been a matter of controversy, due to the electron self-interaction problem. This self-interaction problem has been reputed to cause DFT methods to predict some anionic systems to be unbound relative to the analogous neutral systems.[2,3] Despite this problem, reliable adiabatic electron affinities (AEA) have been predicted using DFT methods.[4−15]

Galbraith and Schaefer[2] tested the severity of this effect by application of DFT to the F and Ne atoms and the F_2 molecule and the three corresponding anions with basis sets of increasing size and did indeed show that DFT could be succesfully applied to anionic sytems even though the HOMO energies obtained from pure DFT functionals do sometimes have positive eigenvalues. Rösch and Trickey offered an interesting response to this study[3] and addressed some topics concerning application of DFT to anionic systems. The electron−electron repulsion term, E_{ee}, derived in the Kohn−Sham formulation of DFT includes the repulsion of an electron with itself and, with an exact nonlocal functional the exchange term, E_{xc}, would precisely cancel out this spurious electron self-interaction. However, all current local approximations of E_{xc}, offer only pointwise descriptions of the density, causing incomplete cancelation. Systems with a high degree of localized electron density or an excess of electrons over protons may be especially susceptible to this failing in the local approximation. In addition, the use of finite basis sets leads to the wrong asymptotic behavior for unbound systems, and this incorrect behavior causes a cancelation of the local approximation, thereby causing an artificial stabilization. Rösch and Trickey also commented that for large molecules in which the electron population is delocalized over the molecule, the electron self-interaction problem would also be delocalized and therefore be less significant. Tschumper and Schaefer showed that as one increases the size from one to two or three heavy atoms, the EA predictions with DFT do not generally improve.[14] But for larger systems, Rienstra-Kiracofe, Graham, and Schaefer showed that delocalization does improve the predicted EA's in the particular case of several organic ring molecules.[13]

Despite the ongoing debate on this topic, recent papers from our group[13,14] and from Curtiss, Redfern, Raghavachari, and Pople[15] show that both pure and hybrid DFT methods provide a relatively accurate means for predicting the adiabatic electon affinities of a wide range of molecular systems that have known experimental electron affinities. Predicting the adiabatic electron affinities (AEA) of molecules presents an interesting challenge to theoretical chemistry. As described by Ziegler and Gutsev,[5] there are many difficulties in calculating the AEA for molecular systems. The geometry and energetics of both the neutral and anionic species must be determined with the computational method, which means that one must utilize a basis set that provides a proper description of both the neutral species and the diffuse nature of the anionic species. Our group has shown[13,14] that Dunning's DZP basis set augmented with diffuse functions, while not adequate for convergent quantum mechanics methods (e.g., coupled-cluster methods), exhibits the needed flexibility and is small enough in size to be applicable to large molecular systems. Also, the AEA is sensitive to subtle changes in correlation energy between the neutral and anionic species. Since DFT provides a computationally tractable means of including correlation energy in a quantum chemical computation, it is ideal for use in predicting the electron affinities of large molecular systems, to which traditional convergent quantum chemical methods (e.g., coupled-cluster theory) are not applicable at this time.

With these factors in mind, the AEA of some medium-sized carbon-based molecules using DFT are presented in the present work. The neutral and anionic species studied include linear carbon clusters C_n ($n = 6-9$), the neutral triacetylene radical (C_6H), tetracyanoethylene (TCNE), 1,1,1-trifluoroacetone enolate (TFAE), and the C_4O radical. All of these molecules have known experimental electron affinities. In addition, we sought to evaluate the performance of DFT in the determination of

† John C. Slater Graduate Fellow. E-mail: sbrown@xerxes.ccqc.uga.edu.

10.1021/jp984354c CCC: $18.00 © 1999 American Chemical Society
Published on Web 04/28/1999

geometric parameters, harmonic vibrational frequencies, and the property differences between the neutral and anionic species.

In this study, the electronic energy, equillibrium geometry, harmonic vibrational frequencies, and zero point vibrational energy (ZPVE) for the neutral and anion of all of the molecules studied were computed with different approximate local density functionals, three pure DFT functionals (BLYP, BP86, and LSDA), and three Hartree−Fock hybrid functionals (B3LYP, B3P86, and BHLYP). The hybrid functionals are formulated in a way that reduces the severity of the electron self-interation problem, and so it is interesting to assess the performance of the various pure and hybrid functionals in predicting the AEA. Discussion of the performance of the various DFT methods for these properties in comparison to each other and to experiment has been included.

In order to provide comparison between previous results from our group, the procedure followed in the previous studies has been preserved[13,14] and a discussion of the accuracy of the various functionals in predicting AEA's for all of the molecules studied has been provided.

II. Theoretical Methods

Total energies, equilibrium geometries, harmonic vibrational frequencies, and ZPVE's were determined for the neutral and anion species for each of the eight molecules studied. Six different exchange-correlation density functionals were used and have been denoted B3LYP, B3P86, BHLYP, BLYP, BP86, and LSDA. The first five are generalized gradient approximations (GGA's) and employ the dynamical correlation functional of Lee, Yang, and Parr (LYP)[16] or that of Perdew (P86)[17,18] in conjunction with one of Becke's exchange functionals: the three-parameter HF/DFT hybrid exchange functional (B3),[19] a modification of the half-and-half HF/DFT hybrid method as impemented in GAUSSIAN 94 (BH),[20] or the 1988 pure DFT exchange functional (B).[21] The sixth density functional scheme used in the study was the standard local-spin-density approximation (LSDA), which employs the 1980 correlation functional of Vosko, Wilk, and Nusair[22] along with the Slater exchange functional.[23−25]

All functionals employed a double-ζ basis set with polarization and diffuse functions, denoted DZP++. It was constructed by augmenting the Huzinaga−Dunning[26,27] set of contracted double-ζ Gaussian functions with one set of *p* polarization functions for each H atom and one set of five *d* polarization functions for each C, N, O, and F atom. ($\alpha_p(H) = 0.75$, $\alpha_d(C) = 0.75$, $\alpha_d(N) = 0.80$, $\alpha_d(O) = 0.85$, $\alpha_d(F) = 1.00$). To complete the DZP++ basis, one even-tempered *s* diffuse function was added to each H atom and a set of even tempered s and p diffuse functions to all other atoms. These "even-tempered" orbital exponents were determined according to the guidelines of Lee and Schaefer.[28] That is, the *s*- or *p*-type diffuse function exponent, $\alpha_{diffuse}$, for a given atom was determined by

$$\alpha_{diffuse} = \frac{1}{2}\left(\frac{\alpha_1}{\alpha_2} + \frac{\alpha_2}{\alpha_3}\right)\alpha_1$$

where α_1 is the smallest, α_2 the second smallest, and α_3 the third smallest Gaussian orbital exponent of the *s*- or *p*-type primitive functions of that atom ($\alpha_s(H) = 0.04415$, $\alpha_s(C) = 0.04302$, $\alpha_p(C) = 0.03629$, $\alpha_s(N) = 0.06029$, $\alpha_p(N) = 0.05148$, $\alpha_s(O) = 0.08227$, $\alpha_p(O) = 0.06508$, $\alpha_s(F) = 0.1049$, $\alpha_p(F) = 0.0826$). All polarization and diffuse orbital exponents were unscaled. There are a total of six DZP++ basis functions per H atom and nineteen per C, N, O, and F atom.

The quantum chemical computations for this study were conducted with the GAUSSIAN 94[29] computational package. Spin unrestricted Kohn−Sham orbitals were used for all computations. Both the neutral and anion geometries were optimized via analytic gradients with each of the six density functionals. Numerical integration of the functionals was carried out using the GAUSSIAN 94[29] default grid consisting of 75 radial shells with 302 angular points per shell. The mass-weighted Hessian matrix, and hence the harmonic vibrational frequencies, were determined analytically for all DFT methods. As outlined in section I, the adiabatic electron affinities for the molecules studied were computed by differences between the total energy of the optimized neutral and the total energy of the corresponding optimized anion.

$$\mathrm{AEA} = E_{neut} - E_{anion} \tag{1}$$

ZPVE-corrected electron affinities were also determined by adding the corresponding harmonic ZPVE to these total energies before subtracting the energy of the anion from that of the neutral.

III. Results and Discussion

A. Linear Carbon Chains, C_n ($n = 6-9$). Linear carbon chains have a wide variety of chemical interests. An understanding of their stuctures and properties is important in soot formation, interstellar chemistry, and understanding the formation of larger carbon clusters.[30] It has been established that carbon clusters with fewer than ten atoms have linear ground state structures,[30] and there is recent evidence that linear carbon clusters with up to 16 atoms exist.[31] There has been a wide range of spectroscopic studies of linear carbon chains performed to learn about their formation and properties.[30,32−38] Individually, C_6,[37−42] C_7,[36,43,44] C_8,[37] and C_9[36,45,46] have been studied for their vibrational and electronic spectra both in the gas phase and in matrix isolation experiments. For a comprehensive overview of the chemistry of small carbon clusters, refer to the recent review by Orden and Saykally.[47] In 1988 Yang, Taylor, Craycraft, Conceicao, Pettiette, Cheshnovsky, and Smalley used anion photoelectron detachment spectrocopy to determine the electron affinities of carbon clusters with up to 30 atoms, including the linear carbon clusters of up to 9 atoms.[34] Three years later Arnold, Bradforth, Kitsopoulos, and Neumark obtained the vibrationally resolved spectrum using the same technique,[32] allowing for the determination of more accurate electron affinities [C_6 (4.185 ± 0.006 eV), C_7 (3.358 ± 0.014 eV), C_8 (4.379 ± 0.006 eV), C_9 (3.684 ± 0.010 eV)]. Both studies show a sharp alternation in the electron affinities between clusters with even and odd numbers of atoms. Also, a number of theoretical investgations have been performed on linear carbon clusters as a whole[35,48−55] and individually (C_6,[56−58] C_8,[57] and C_9[59,60]).

Figure 1 defines the geometric parameters for the linear carbon clusters studied, and the optimized parameters for both neutral and anionic species are presented in Table 1. Optimized geometries calculated for the neutral species at the CCSD(T)/cc-pVDZ level of theory by Martin and Taylor[51] have been provided for comparison. For all species, the carbon−carbon bond distances indicate that the linear chains are cumulene-like in nature. The overall agreement between the coupled cluster geometries and our optimized parameters is within 2%, with the BHLYP functional consistently providing the poorest agreement. The pure DFT functionals tend to predict slightly longer bond distances than the hybrid methods. The geometry

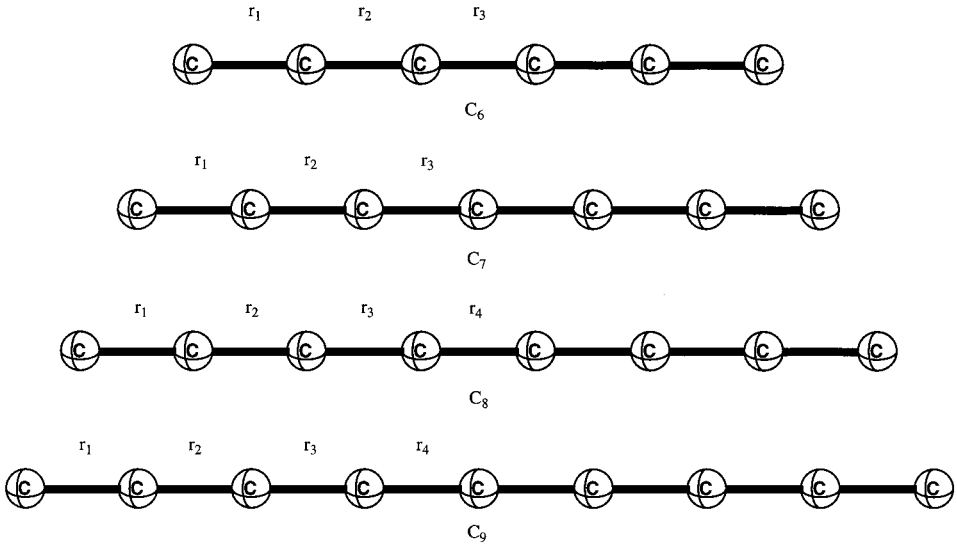

Figure 1. Geometric parameters for the linear carbon chain molecules. Parameters apply to both the neutral and anionic species. Optimized geometries are given in Table 1.

TABLE 1: Optimized Geometries[a] for Linear Carbon Clusters C_n ($n = 6-9$) and Their Anions[b]

	elec symm		B3LYP		B3P86		BHLYP		BLYP		BP86		LSDA		CCSD(T)[c]
	neut	anion	neut	anion	neut	anion	neut	anion	neut	anion	neut	anion	neut	anion	neut
C_6	$^3\Sigma_g^-$	$2\Pi_u$													
r_1			1.313	1.285	1.312	1.284	1.300	1.269	1.327	1.300	1.328	1.300	1.316	1.290	1.3257
r_2			1.300	1.338	1.297	1.335	1.288	1.333	1.311	1.344	1.309	1.342	1.301	1.331	1.3092
r_3			1.286	1.263	1.284	1.262	1.276	1.247	1.296	1.277	1.295	1.277	1.286	1.269	1.2973
C_7	$^1\Sigma_g^+$	$2\Pi_g$													
r_1			1.299	1.290	1.298	1.289	1.284	1.276	1.313	1.305	1.314	1.305	1.304	1.295	1.3164
r_2			1.299	1.319	1.297	1.317	1.288	1.311	1.309	1.327	1.308	1.326	1.299	1.316	1.3097
r_3			1.284	1.289	1.282	1.287	1.273	1.279	1.294	1.299	1.293	1.298	1.285	1.290	1.2958
C_8	$^1\Sigma_g^-$	$2\Pi_g$													
r_1			1.308	1.284	1.307	1.283	1.295	1.268	1.321	1.299	1.322	1.300	1.311	1.290	1.3207
r_2			1.301	1.333	1.298	1.330	1.289	1.329	1.311	1.339	1.310	1.337	1.301	1.327	1.3111
r_3			1.284	1.263	1.282	1.262	1.274	1.247	1.294	1.278	1.293	1.278	1.285	1.270	1.2957
r_4			1.292	1.326	1.289	1.323	1.281	1.323	1.302	1.329	1.300	1.327	1.293	1.318	1.3018
C_9	$^1\Sigma_g^+$	$2\Pi_u$													
r_1			1.298	1.288	1.297	1.286	1.282	1.273	1.312	1.302	1.313	1.303	1.303	1.292	1.3164
r_2			1.301	1.322	1.299	1.319	1.291	1.314	1.311	1.329	1.310	1.328	1.300	1.318	1.3121
$r3$			1.282	1.280	1.280	1.278	1.270	1.269	1.292	1.291	1.291	1.290	1.283	1.282	1.2947
r_4			1.288	1.298	1.285	1.295	1.277	1.289	1.297	1.306	1.296	1.305	1.288	1.296	1.2993

[a] Bond distances are given in Å. [b] Geometric parameters correspond to those shown in Figure 1. [c] See ref 51.

change between the neutral and anion shows a shift from the cumulene-like structure, in which the alternation between adjacent bonds is minimal, to a slightly more polyacetylene-like structure in which the alternation is slightly more prominent. This can be qualitatively understood by examining the singly occupied molecular orbital (SOMO) for the anionic species, because addition of an electron into this orbital is the main difference between the two species. The anion SOMO's for the linear carbon chains studied here are given in Figure 2. In the even-numbered chains, C_6 and C_8, the anion SOMO provides strong bonding and antibonding (r_2 for C_6; r_2 and r_4 for C_8) character between alternating bonds, and there is a corresponding decrease in bond distance for the bonding interactions (r_1 and r_3 for C_6 and C_8) and an increase for the antibonding interactions (r_2 for C6; r_2 and r_4 for C_8). For the odd-numbered chains, C_7 and C_9, the SOMO provides strong bonding character between the two terminal carbons, hence shortening the bond distance r_1 in both cases. Between the next two carbons there is an antibonding interaction and a lengthening of the bond distance r_2 in the case of C_7, and in the case of C_9 there is additional antibonding interaction, causing a lengthening in both r_2 and r_4. There is slight shortening in r_3 in both cases that can be attributed to some weak bonding interactions between the adjacent carbons.

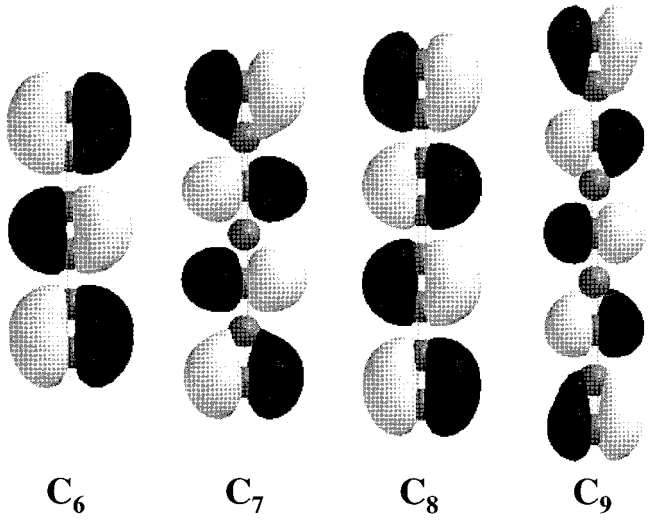

Figure 2. SOMO's for the linear carbon chain anions C_n ($n = 6-9$).

TABLE 2: Harmonic Vibrational Frequencies ω_e (in cm^{-1}) for Linear C_6 and Its Anion

mode			B3LYP		BLYP		BP86		expt	
neut	anion	symm	neut	anion	neut	anion	neut	anion	neut	anion
ω_1	ω_1	Σ_g	2152	2153	2069	2067	2090	2087	2089 ± 50^c	2086 ± 2^d
ω_2	ω_2	Σ_g	1709	1830	1638	1744	1645	1752	1694 ± 50^c	1775 ± 2^d
ω_3	ω_3	Σ_g	660	645	635	623	638	627	637 ± 50^c	634 ± 2^d
ω_4	ω_4	Σ_u	1996	1993	1918	1916	1931	1930	1952.5[e]	1936.7 ± 0.2^d
ω_5	ω_5	Σ_u	1213	1200	1161	1158	1166	1166	1197.3[e]	
ω_6	ω_{6a}	$(\Pi_g)^a$	508	561	477	532	475	530		
ω_6	ω_{6b}	$(\Pi_g)^b$	508	503	477	467	475	466		
ω_7	ω_{7a}	$(\Pi_g)^a$	223	253	200	236	190	230	246 ± 50^c	
ω_7	ω_{7b}	$(\Pi_g)^b$	223	263	200	254	190	253	246 ± 50^c	
ω_8	ω_{8a}	$(\Pi_u)^a$	386	411	348	382	341	378		
ω_8	ω_{8b}	$(\Pi_u)^b$	386	449	348	430	341	434		
ω_9	ω_{9a}	$(\Pi_u)^a$	115	125	108	120	105	118	90 ± 50^c	
ω_9	ω_{9b}	$(\Pi_u)^b$	115	128	108	124	105	123	90 ± 50^c	

[a] Bending is in plane with respect to the SOMO. [b] Bending is out of plane with repect to the SOMO. [c] Photoelectron spectroscopy: see ref 37. [d] Matrix isolation IR: see ref 38. [e] Matrix isolation IR: see ref 35.

TABLE 3: Harmonic Vibrational Frequencies ω_e (in cm^{-1}) for Linear C_7 and Its Anion

mode			B3LYP		BLYP		BP86		expt	
neut	anion	symm	neut	anion	neut	anion	neut	anion	neut	anion
ω_1	ω_1	Σ_g	2183	2037	2097	1978	2112	1996		
ω_2	ω_2	Σ_g	1586	1580	1520	1518	1527	1525		
ω_3	ω_3	Σ_g	579	566	558	547	561	551	548 ± 90^c	
ω_4	ω_4	Σ_u	2219	1955	2157	1938	2178	1961	2127.8[d]	
ω_5	ω_5	Σ_u	1955	1787	1873	1782	1883	1797	1894.3[d]	1734.8[e]
ω_6	ω_6	Σ_u	1101	1070	1057	1032	1062	1038		
ω_7	ω_{7a}	$(\Pi_g)^a$	551	560	520	533	524	537	496 ± 110^c	
ω_7	ω_{7b}	$(\Pi_g)^b$	551	455	520	431	524	436		
ω_8	ω_{8a}	$(\Pi_g)^a$	191	210	184	203	178	200		
ω_8	ω_{8b}	$(\Pi_g)^b$	191	210	184	202	178	203		
ω_9	ω_{9a}	$(\Pi_u)^a$	668	673	626	640	620	634		
ω_9	ω_{9b}	$(\Pi_u)^b$	668	552	626	520	620	516		
ω_{10}	ω_{10a}	$(\Pi_u)^a$	289	314	282	308	277	306		
ω_{10}	ω_{10b}	$(\Pi_u)^b$	289	372	282	357	277	357		
ω_{11}	ω_{11a}	$(\Pi_u)^a$	90	95	88	93	86	92		
ω_{11}	ω_{11b}	$(\Pi_u)^b$	90	95	88	93	86	92		

[a] Bending is in plane with respect to the SOMO. [b] Bending is out of plane with repect to the SOMO. [c] Photoelectron spectrocopy: ref 32. [d] Matrix isolation IR: ref 44. [e] Matrix isolation IR: ref 35.

TABLE 4: Harmonic Vibrational Frequencies ω_e (in cm^{-1}) for Linear C_8 and Its Anion

mode			B3LYP		BLYP		BP86		expt	
neut	anion	symm	neut	anion	neut	anion	neut	anion	neut	anion
ω_1	ω_1	Σ_g	2108	2126	2041	2051	2065	2074	1977 ± 10^c	
ω_2	ω_2	Σ_g	1998	1993	1921	1911	1934	1924		
ω_3	ω_3	Σ_g	1384	1360	1329	1318	1336	1326	1361 ± 10^c	
ω_4	ω_4	Σ_g	508	498	490	482	493	486	605 ± 10^c	
ω_5	ω_5	Σ_u	2131	2136	2059	2059	2076	2076	2071.5[d]	
ω_6	ω_6	Σ_u	1744	1850	1677	1767	1684	1774	1710.5[d]	
ω_7	ω_7	Σ_u	964	947	927	915	931	921		
ω_8	ω_{8a}	$(\Pi_g)^a$	768	777	723	739	708	725		
ω_8	ω_{8b}	$(\Pi_g)^b$	768	752	723	705	708	695		
ω_9	ω_{9a}	$(\Pi_g)^a$	427	442	399	419	394	417		
ω_9	ω_{9b}	$(\Pi_g)^b$	427	467	399	447	394	450		
ω_{10}	ω_{10a}	$(\Pi_g)^a$	165	179	155	171	150	167		
ω_{10}	ω_{10b}	$(\Pi_g)^b$	165	185	155	179	150	178		
ω_{11}	ω_{11a}	$(\Pi_u)^a$	621	639	582	602	585	607		
ω_{11}	ω_{11b}	$(\Pi_u)^b$	621	608	582	568	585	574		
ω_{12}	ω_{12a}	$(\Pi_u)^a$	264	285	244	269	237	264		
ω_{12}	ω_{12b}	$(\Pi_u)^b$	264	294	244	287	237	287		
ω_{13}	ω_{13a}	$(\Pi_u)^a$	73	77	71	75	70	74		
ω_{13}	ω_{13b}	$(\Pi_u)^b$	73	78	71	76	70	76		

[a] Bending is in plane with respect to the SOMO. [b] Bending is out of plane with repect to the SOMO. [c] Photoelectron spectroscopy: see ref 37. [d] Matrix isolation IR: see ref 38.

Harmonic vibrational frequencies are reported in Tables 2−5 and Tables XVII−XX (Supporting Information) for all of the linear carbon clusters studied. Also listed are assignments to experimental fundamentals for both neutral and anionic species from a variety of research where values are available. While discussion of the various experiments is not pertinent to this research, it can be seen that our estimations provide agreement within 4−5% of experiment, with BHLYP once again showing

TABLE 5: Harmonic Vibrational Frequencies ω_e (in cm^{-1}) for Linear C_9 and Its Anion

mode			B3LYP		BLYP		BP86		expt	
neut	anion	symm	neut	anion	neut	anion	neut	anion	neut	anion
ω_1	ω_1	Σ_g	2241	2111	2159	2061	2178	2082	2241	
ω_2	ω_2	Σ_g	1943	1909	1863	1835	1873	1846		
ω_3	ω_3	Σ_g	1275	1246	1225	1204	1232	1211	1258 ± 50[c]	
ω_4	ω_4	Σ_g	457	449	441	435	444	438	484 ± 48[c]	
ω_5	ω_5	Σ_u	2183	2049	2123	1993	2146	2012	2079.673[d]	
ω_6	ω_6	Σ_u	2094	1771	2024	1841	2039	1866	2014.278[d]	1686.7[f]
ω_7	ω_7	Σ_u	1647	1636	1582	1582	1590	1590	1601[d]	1583.3[f]
ω_8	ω_8	Σ_u	882	862	849	832	853	837		
ω_9	ω_{9a}	$(\Pi_g)^a$	804	811	762	769	757	769		
ω_9	ω_{9b}	$(\Pi_g)^b$	804	746	762	703	757	704		
ω_{10}	ω_{10a}	$(\Pi_g)^a$	351	367	342	359	338	357		
ω_{10}	ω_{10b}	$(\Pi_g)^b$	351	403	342	388	338	388		
ω_{11}	ω_{11a}	$(\Pi_g)^a$	141	150	137	146	133	144		
ω_{11}	ω_{11b}	$(\Pi_g)^b$	141	154	137	149	133	148		
ω_{12}	ω_{12a}	$(\Pi_u)^a$	904	936	872	898	806	853		
ω_{12}	ω_{12b}	$(\Pi_u)^b$	904	909	872	867	806	832		
ω_{13}	ω_{13a}	$(\Pi_u)^a$	580	597	554	571	545	567		
ω_{13}	ω_{13b}	$(\Pi_u)^b$	580	526	554	504	545	502		
ω_{14}	ω_{14a}	$(\Pi_u)^a$	226	245	218	238	212	234		
ω_{14}	ω_{14b}	$(\Pi_u)^b$	226	260	218	251	212	250		
ω_{15}	ω_{15a}	$(\Pi_u)^a$	59	62	59	61	57	61	30 ± 20[e]	
ω_{15}	ω_{15b}	$(\Pi_u)^b$	59	63	59	62	57	62	30 ± 20[e]	

[a] Bending is in plane with respect to the SOMO. [b] Bending is out of plane with repect to the SOMO. [c] Photoelectron spectroscopy: see ref 32. [d] Matrix isolation IR: see ref 45. [e] Gas-phase IR: see ref 46. [f] Matrix isolation IR: see ref 35.

the poorest agreement overall (7.0%). The BLYP functional provides the best agreement with an absolute percent difference of 3.6%. It should be noted that the ω_9 of C6 and ω_{15} of C_9 have been ommitted in the statistics due to the large experimental error involved in their determination. Overall the errors [BLYP (3.6%), BP86 (3.7%), B3LYP (4.4%), B3P86 (5.2%), LSDA (5.2%), and BHLYP (7.0%)] for all functionals for these linear carbon chains are of the order of magnitude of neglected effects due to anharmonicity.

AEA electron affinities estimated with B3LYP, BHLYP, BLYP, and BP86 (see Table 16) show agreement with the values measured by Arnold et al.[32] within 7% for C_6 through C_9. The BP86 functional overall provides values closest to experiment with an average absolute error of 0.10 eV and the B3P86 functional provides the overall worst agreement (average absolute error: 0.52 eV). The LSDA functional also provides poor agreement (average absolute error: 0.50 eV), which is expected since this functional should suffer most from the local approximation. Since the optimized geometries show cumulene-like structures, the electron density for these linear carbon clusters in both the neutral and anion species should be fairly uniformly distributed throughout the molecule, and therefore it is expected that the local DFT methods should provide good descriptions of these molecules' electron densities. ZPVE corrections to the energies tend to raise the estimated AEA's by 0.01−0.03 eV in the case of the even-numbered chains but lower the AEA's by 0.01−0.06 eV for the odd-numbered chains. This phenomenon may be atributed qualitatively to the SOMO's shown in Figure 2. If partitioning of the ZPVE into stretching and bending contributions is performed, it is clear that the major portion of the ZPVE is due to the stretching vibrations. The shift in AEA is in turn governed by the shift in the stretching frequencies between the neutral and anionic species, which are a result of the shifting in bond distances between the two species. As shown before, the geomtery change between the neutral and anionic species can be correlated with the character of the SOMO of the anion. There is a trend in the bonding character between the even-numbered and odd-numbered carbon chains in that as an atom is added to the even-numbered chain, the SOMO gains an additional node (e.g., C_6 has two nodes and C_7 has three). Additional nodes imply that the SOMO is more antibonding in character, and an overall weakening of the σ bonding framework will occur from addition of an electron into this orbital. In the odd-numbered chains there will be a lowering of E_0 relative to the neutral species and so a lowering of the AEA will occur. In the even-numbered chains, the anion is produced through addition of an electron into a bonding orbital and this will raise the ZPVE of the anion, thereby raising the AEA. A qualitative illustration of this phenomenon is provided in Figure 3.

B. Triacetylene (C_6H). The C_6H radical has been detected in the interstellar medium and may exist in the diffuse interstellar bands.[61] The ground state of the radical has been established as $^2\Pi$, and theoretical studies have shown that there is a low-lying $^2\Sigma^+$ state.[62−67] It is only recently that this low-lying $^2\Sigma^+$ has been observed experimentally.[68] In 1994, Natterer, Koch, Schröder, Goldberg, and Schwarz utilized thermodynamic studies in conjunction with mass spectrometry to determine the electron affinity of C_6H as 3.69 ± 0.05. Recently, Taylor, Xu, and Neumark performed photoelectron spectroscopy on triacetylene as well as a number of other acetylenic linear carbon chain radicals.[68] From this study, the electron affinity of C_6H was determined to be 3.809 ± 0.015.

Optimized linear geometries for the neutral radical and closed shell anion are provided in Table 6. (refer to Figure 4 for geometric parameters). For the anion, all functionals predict a linear structure to be the global minimum, but for the neutral species only the three Hartree−Fock hybrid functionals show this same result. The pure local DFT functionals predict a slightly bent structure with the linear structure possessing an imaginary vibrational mode coresponding to the θ_1 bending in the neutral radical species (BLYP: 69i cm^{-1}, BP86: 168i cm^{-1}, LSDA: 527i cm^{-1}). In terms of predicting electron affinities, the energy differences between the linear and the bent structures for the pure functionals are as follows: BLYP (0.00012 eV), BP86 (0.0021 eV), and LSDA (0.015 eV). Also the values of θ_1 are provided in Table 6 to show the deviation from linearity where appropriate. As can be seen, even for the LSDA

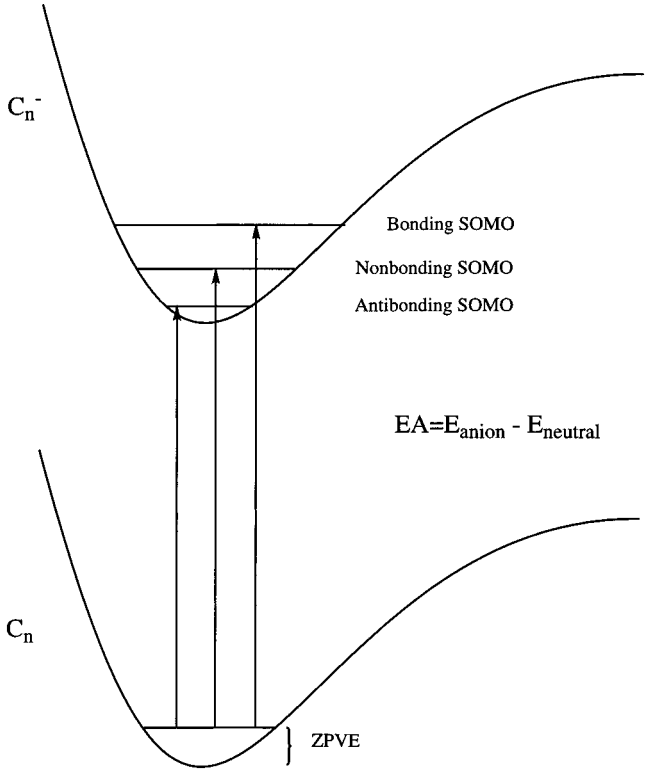

Figure 3. Qualitative representation of the effect that the character of the SOMO has on the zero point vibrational energy (ZPVE) correction for anionic species relative to the neutral. Since, in the linear carbon chain molecules, the major portion of the vibrational energy is due to stretching vibrations, the zero point energy will vary depending on the σ character of the SOMO. In the case of the SOMO being nonbonding, the ZPVE should be about the same for the anion as for the neutral. In the case of an antibonding SOMO there is a lowering of the ZPVE with respect to the neutral due to the decrease of stability in the bonding framework. This would cause a decrease in the EA with ZPVE correction relative to the AEA. In the case of a bonding SOMO, the opposite is true due to a relative increase in the stability of the bonding framework. This effect can be seen in Table 16 for the linear carbon chain molecules in that the even-numbered chains have a bonding SOMO and the odd-numbered chains have an antibonding SOMO.

functional, which exhibits the largest deviation from linearity, the energy difference between the two structures is only 0.015 eV. The experimental error from Taylor et al. is $\pm$0.015 eV,[68] and therefore, it is inconsequential as to which structure is used for the determination of the AEA. So with this in mind, the optimized geometries reported in Table 6, the harmonic vibrational frequencies in Table 7 and Table XXI (Supporting Information), and the calculated AEA's in Table 16 include only values determined from linear structures.

Harmonic vibrational frequencies obtained the DFT functionals for the neutral radical and anionic species are given in Table 7 and Table XXI (Supporting Information). Once again it is important to note that the frequencies provided are for only the linear geometries, and hence the neutral species include an imaginary mode with the pure DFT functionals. The only experimentally assigned mode is the vibrational mode that corresponds to the C≡C stretch closest to the hydrogen in the neutral radical. This was first assigned by Doyle, Shen, Rittby, and Graham[69] to 1953.4 cm^{-1} from argon matrix Fourier transform infrared spectrocopy (FTIR) and an empirical force constant analysis. Later Forney et al. made a tenative assignment at 1962.2 cm^{-1} from neon matrix electron absorbtion spectroscopy.[39] If the assigment of the experimental mode is attributed to the C≡C stretch closest to the hydrogen (i.e., the stretching of r_5) then (from an analysis of the contribution of the internal coordinates of the molecule to each mode) this corresponds to the ω_3 mode. To further examine the assignment, isotope shifts were calclulated for the C_6D and $^{13}C_6H$ isotopomers and compared with the experimentally determined isotope shifts given by Doyle et al.[69] This analysis is summarized in Table 8 and noting that the average agreement between the DFT harmonic frequencies with the various functionals and the experimental fundemental is 5.5%, our results strongly support the assignment made by experiment.

The calculated AEA's using the six DFT functionals employed are given in Table 16. The experimental value of Taylor et al.[68] is provided for comparison. The BP86 functional shows the best agreement with the experimental value, along with B3LYP also showing good agreement. The worst agreement is given by the LSDA functional, which once again would be expected due to the local nature of the functional. The functionals may be ranked in order according to their deviations from experiment [BP86 (0.12 eV), B3LYP (−0.15 eV), BHLYP (−0.33 eV), BLYP (−0.36 eV), B3P86 (0.43 eV), LSDA (0.56 eV)]. ZPVE corrections show a 0.01−0.03 eV increase in the AEA.

C. Tetracyanoethylene. Tetracyanoethylene (TCNE), a dienophile in many Diels−Alder reactions,[70,71] has many applications in organic chemistry[72] and organometallic chemistry.[73] The tetracyanoethylene radical anion is an important component in many magnetic compounds.[74] Theoretically, TCNE is an interesting model for investigating chemical reactivity,[75] chemical bonding,[76−78] and electron donor acceptor (EDA) complexes.[76−81]

Geometric parameters for TCNE and its anion are shown in Figure 5. Our optimized geometries for both the neutral and its radical anion are reported in Table 9. Harmonic vibrational frequencies for both species are given in Table 10 and Table XXII (Supporting Information). We have compared our TCNE neutral geometries to the experimental neutron diffraction data of Becker, Coppens, and Ross.[82] The BHLYP functional predicts bond distances within experimental error for r_1 and r_2, and is only 0.01 Å below experiment for r_3. The other hybrid functionals predict slightly longer bond lengths but are also quite close to the experimental data. The three pure DFT functionals exhibit markedly worse bond-length agreement. For bond angles, all six functionals are in close agreement with each other and are within a degree of the experimental values. It is interesting to note an earlier experimental geometry given by Hope,[83] which was determined using the gas-phase electron diffraction method. Hope's bond distances are all just slightly longer than Becker et al., by 0.004 Å at most.

For the TCNE anion, agreement with the experimental X-ray diffraction data of Dixon and Miller[84] is worse than with neutral TCNE. Experimentally, the anion r_1 distance is seen to increase over the value observed for the parent neutral. Our results also show a corresponding increase in length, but overestimate the experimental results by at least 0.03 Å. Agreement for r_2 is better, with all functionals except LSDA being within 0.01 Å of experiment. For r_3, every functional shows an increase in length over the neutral, whereas experiment shows a decrease. It is possible that DFT is "resisting" localizing electron density about the C−N triple bond. On the other hand, Dixon and Miller do note that determining this C−N distance in X-ray diffraction experiments is difficult. Furthermore, it is always possible that the counterion in the crystal causes significant deviations with respect to the free anion structure. As with the neutral, bond angles for the anion are within 1° of experimental results.

TABLE 6: Optimized Geometries[a] for Linear C_6H and Its Anion[b]

	B3LYP		B3P86		BHLYP		BLYP		BP86		LSDA	
	neut	anion	neut	anion	neut	anion	neut	anion	neut	anion	neut	anion
r_1	1.299	1.270	1.298	1.269	1.284	1.252	1.314	1.285	1.314	1.286	1.304	1.276
r_2	1.327	1.357	1.324	1.353	1.327	1.359	1.331	1.358	1.330	1.357	1.319	1.345
r_3	1.256	1.246	1.254	1.245	1.236	1.227	1.272	1.263	1.271	1.263	1.265	1.256
r_4	1.348	1.362	1.344	1.358	1.353	1.366	1.346	1.361	1.344	1.359	1.333	1.347
r_5	1.231	1.233	1.230	1.232	1.213	1.215	1.247	1.249	1.247	1.249	1.241	1.243
r_6	1.071	1.067	1.071	1.067	1.064	1.060	1.077	1.073	1.079	1.075	1.081	1.076
θ_1[c]							176.2		171.9		168.0	

[a] Bond distances are given in Å and bond angles are given in deg. [b] The geometries of both the neutral ($^2\Pi$) and the anion ($^1\Sigma$) are given for each method. Geometric parameters correspond to those shown in Figure 4. [c] Only if the angle differs from linearity.

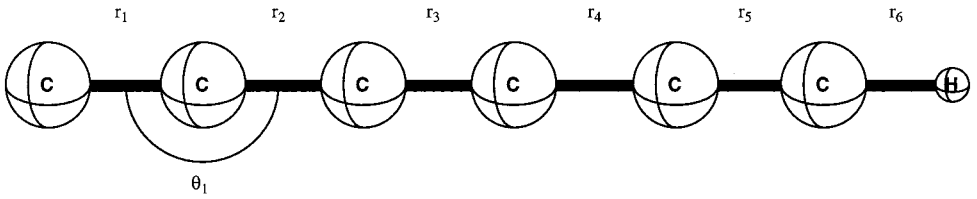

Figure 4. Geometric parameters for the C_6H radical and its anion. Optimized geometries are given in Table 9.

TABLE 7: Harmonic Vibrational Frequencies ω_e (in cm^{-1}) for Linear C_6H and Its Anion

mode			B3LYP		BLYP		BP86		expt	
neut	anion	symm	neut	anion	neut	anion	neut	anion	neut	anion
ω_1	ω_1	Σ	3448	3477	3372	3399	3376	3403		
ω_2	ω_2	Σ	2109	2204	2056	2121	2074	2140		
ω_3	ω_3	Σ	2080	2118	2011	2033	2024	2047	1953.4[c]	
ω_4	ω_4	Σ	1872	1951	1790	1859	1798	1867		
ω_5	ω_5	Σ	1210	1193	1182	1167	1190	1176		
ω_6	ω_6	Σ	642	633	627	617	631	622		
ω_{7a}	ω_7	$(\Pi)^a$	561	576	524	544	521	544		
ω_{7b}	ω_7	$(\Pi)^b$	679	576	622	544	627	544		
ω_{8a}	ω_8	$(\Pi)^a$	519	498	479	474	480	476		
ω_{8b}	ω_8	$(\Pi)^b$	553	498	501	474	500	476		
ω_{9a}	ω_9	$(\Pi)^a$	445	437	385	319	399	336		
ω_{9b}	ω_9	$(\Pi)^b$	396	437	357	319	351	336		
ω_{10a}	ω_{10}	$(\Pi)^a$	255	272	245	264	244	265		
ω_{10b}	ω_{10}	$(\Pi)^b$	214	272	143	264	131	265		
ω_{11a}	ω_{11}	$(\Pi)^a$	120	123	116	120	115	120		
ω_{11b}	ω_{11}	$(\Pi)^b$	110	123	-69	120	-168	120		

[a] Bending is in plane with respect to the SOMO. [b] Bending is out of plane with respect to the SOMO. [c] FTIR: see ref 39.

TABLE 8: Theoretical Isotope Shifts (in cm^{-1}) for the Harmonic Vibrational Frequency ω_3 of Linear Neutral C_6H

method	C_6H	$\Delta\omega_3$ C_6D	$\Delta\omega_3$ $^{13}C_6H$[a]
B3LYP	2109	78	78
B3P86	2129	79	78
BHLYP	2185	65	83
BLYP	2056	68	75
BP86	2074	69	76
LSDA	2144	44	51
expt(ν_2)[b]	1953.4	91.0	70.4

[a] Refers to C_6H with all of the carbons substituted by ^{13}C. [b] See ref 69.

Proper assignment of the IR and Raman bands for neutral TCNE has proven to be an interesting challenge for experimentalists. The IR and Raman spectra of TCNE have been reported several times.[85−91] A thorough discussion of all these previous results is beyond the scope of this paper. However, we present here a comparison of our harmonic vibrational frequency results, shown in Table XXII, to the assignments of Hinkel and Devlin,[85] Miller et. al.,[86] and Michaelian, Rieckhoff, and Voigt (MRV).[87,88]

While our reported frequencies are harmonic, we have shown that the functionals employed in this study often obtain satisfactory agreement with experimental fundamentals to within

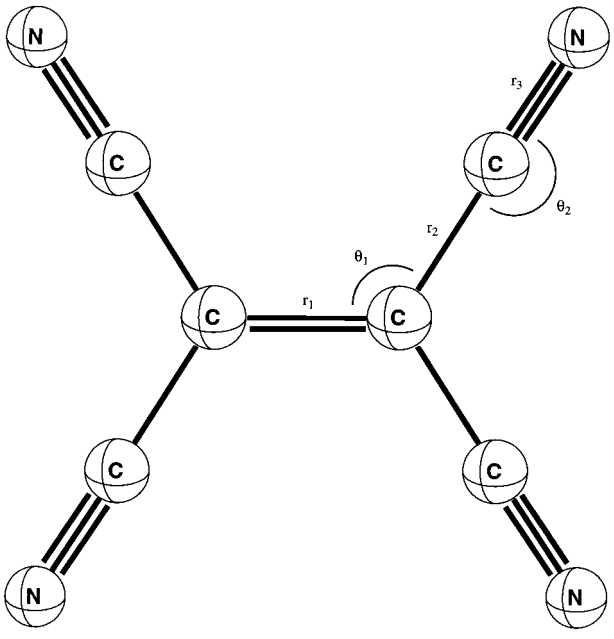

Figure 5. Geometric parameters for tetracyanoethylene (TCNE) and its anion. Optimized geometries are given in Table 9.

TABLE 9: Optimized Geometries for Tetracyanoethylene and Its Negative Ion (Both D_{2h} Symmetry)[a]

	B3LYP		B3P86		BHLYP		BLYP		BP86		LSDA		expt	
	neut	anion	neut	anion	neut	anion	neut	anion	neut	anion	neut	anion	neut[a]	anion[b]
r_1	1.376	1.444	1.372	1.438	1.354	1.429	1.396	1.460	1.393	1.454	1.380	1.436	1.355(2)	1.392(9)
r_2	1.435	1.417	1.429	1.413	1.432	1.412	1.439	1.424	1.435	1.420	1.417	1.404	1.431(1)	1.417(2)
r_3	1.167	1.176	1.166	1.174	1.150	1.159	1.182	1.190	1.182	1.190	1.174	1.182	1.160(1)	1.140(4)
θ_1	121.7	121.8	121.5	121.8	121.7	121.8	121.7	121.8	121.5	121.8	121.1	121.5	121.945(40)	121.15
θ_2	178.9	179.1	179.0	179.1	179.1	179.2	178.7	178.9	178.8	179.0	179.3	179.3	177.93(7)	179.9

[a] Both the neutral (^1A_g) and anion ($^2B_{2g}$) geometries are given for each method. (Bond lengths are in Å and bond angles in degrees.) Geometric parameters correspond to those shown in Figure 4. [b] Neutron diffraction analysis: ref 82. [c] X-ray diffraction analysis of $[Fe(CsMe_5)_2]^{\bullet+}[TNCE]^{\bullet-}$ salt: ref 84.

TABLE 10: Harmonic Vibrational Frequencies ω_e (in cm^{-1}) for Tetracyanoethylene and Its Anion

		B3LYP		BLYP		BP86		expt			
mode	symm	neut	anion	neut	anion	neut	anion	neut[a]	neut[b]	neut[c]	anion[d]
ω_1	A_g	2314	2262	2198	2154	2211	2171	2235	2236	2236	2200
ω_2	A_g	1591	1443	1495	1365	1515	1389	1569	1569	1567	1392
ω_3	A_g	606	630	507	607	589	608	535	679	592	532
ω_4	A_g	530	526	587	505	509	509	490	541	532?	464
ω_5	A_g	116	126	112	121	110	119	130	127	134, 150[e]	
ω_6	B_{1g}	380	457	364	433	364	435		416?	360	
ω_7	B_{2g}	746	629	719	611	710	604		596?	674	
ω_8	B_{2g}	273	288	264	281	262	279		360?	251	
ω_9	B_{3g}	2316	2199	2196	2097	2211	2115	2247	2247	2247	
ω_{10}	B_{3g}	1300	1293	1248	1249	1262	1264	1282	1280	1278	
ω_{11}	B_{3g}	515	534	497	513	499	515	510?	510	508	
ω_{12}	B_{3g}	249	256	239	246	238	245	254	253	251	
ω_{13}	A_u	471	464	451	440	453	442			410	
ω_{14}	A_u	77	52	73	51	73	51			88[f]	
ω_{15}	B_{1u}	2340	2255	2226	2151	2240	2168	2230	2260		
ω_{16}	B_{1u}	982	1002	951	969	957	976	958	958		970
ω_{17}	B_{1u}	589	614	568	591	568	590	579	578		
ω_{18}	B_{1u}	145	155	139	149	137	148	165	165	159, 166[d]	
ω_{19}	B_{2u}	2320	2209	2201	2107	2217	2126	2263	2228		
ω_{20}	B_{2u}	1164	1189	1120	1149	1139	1168	1155	1155		1187
ω_{21}	B_{2u}	431	463	410	439	408	438	443	426		
ω_{22}	B_{2u}	104	107	100	104	97	101	119?	119	119	
ω_{23}	B_{3u}	585	544	562	517	560	517		554?	555	
ω_{24}	B_{3u}	158	155	153	153	150	151		442?	180?	

[a] IR and Raman spectra: ref 85. [b] IR and Raman spectra: ref 86. [c] Analysis of IR and Raman spectra: refs 87, and 88. [d] Analysis of IR and Raman spectra: refs 87, and 88. [e] Davydov splitting. [f] Suggested, see ref 88.

a 4% error.[13] And while the likely difficulty of properly describing the triple bonds in TCNE further cautions one against relying too heavily on the interpretation of our DFT-predicted frequencies, overall trends among the functionals with respect to experiment should be able to offer valuable insight into the difficult experimental assignments.

Examining modes $\omega_1-\omega_2$, $\omega_9-\omega_{12}$, $\omega_{15}-\omega_{17}$, and $\omega_{19}-\omega_{21}$, in which we see close agreement among experimental results, we note that B3LYP tends to overestimate experimental results, whereas BP86 underestimates experiment. Thus the two functionals may be thought of as providing a bracket about the experimental result. With this assumption, we can make some observations where the experimental results are less clear. Specifically, the assignment of 592 cm^{-1} to ω_3 by MRV appears to be the best. MRV's assignment for ω_6 also appears to be good, and their assignments for ω_7 and ω_8 are reasonable. Our results also support MRV in their assignment of 180 cm^{-1} for ω_{24}. Our harmonic frequencies for the spectroscopically inactive a_u modes support MRV's assignment of 410 cm^{-1} for ω_{13}, and their suggested value of 88 cm^{-1} for ω_{14} is reasonable. Finally, we should note that six fundamentals reported for the TCNE anion by Hinkel and Devlin[85] are in reasonable agreement with our predicted anion frequencies.

Early experimental results for the electron affinity of TCNE ranged from 2.03 to 2.88 eV.[92-96] However, the most recent and presumably best experimental result (obtained via ion/molecule reaction equilibria) places the electron affinity at 3.17 $\pm$ 0.20 eV.[97,98] Previous theoretical predictions range from 2.63 to 3.11;[78,99-102] however, none were obtained with a highly correlated level of theory.

Our results all overestimate the experimental electron affinity, although the BLYP prediction is within experimental error. Similar overestimations were observed in our previous study on the electron affinity of *o*-benzyne and maleic anhydride.[13] Our EA's are lowered by about 0.02 eV with ZPVE corrections, thus bringing them closer to experiment. It was proposed that the highly localized electron density in *o*-benzyne and maleic anhydride increased the error of the DFT predictions. Because TCNE has four triple bonds, it may also be that the increased electron density associated with these bonds is causing similar overestimations of the experimental EA. If this is so, it seems that the BLYP prediction for TCNE is the result of a fortuitous cancelation in error between BLYP's tendency to underpredict EAs, and the overestimation caused by the excess localized density in TCNE. Nevertheless, the large experimental error does not allow us to exclude the possibility that the experimental value is too low. A redetermination of the electron affinity of TCNE would be valuable.

D. 1,1,1-Trifluoroacetone Enolate. A lower limit for the electron affinity of the 1,1,1-trifluoroacetone enolate (TFAE) radical was measured with an ion cyclotron resonance (ICR) spectrometer by Zimmerman, Reed, and Brauman in 1977 and

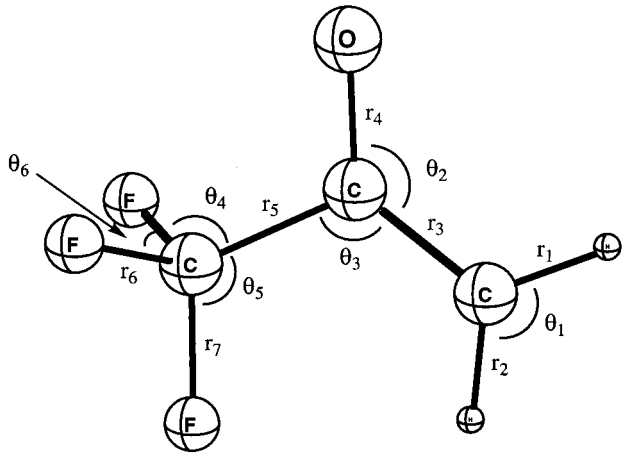

Figure 6. Geometric parameters for 1,1,1-trifluoroacetone enolate (TFAE) and its anion. Optimized geometries are given in Table 11.

given to be 2.58 ± 0.13 eV.[103] Later, Brinkman, Berger, Marks, and Brauman improved upon the previous result and placed the EA at 2.625 ± 0.010 eV.[104]

We investigated two conformations of the TFAE radical and the TFAE anion. Both conformations are of C_s symmetry, with conformation A corresponding to the structure shown in Figure 6, while the other, B, is similar to A, except that the CF_3 group is rotated 180° with respect to A. In the anion, with the B3LYP functional, conformation B is a transition state with an imaginary vibrational frequency of 61i, which corresponds to rotation of the CF_3 group. This transition state lies 2.03 kcal/mol higher than conformation A. Thus we optimized only conformation A for the anion with the remaining five functionals and found it to be a minimum in each case.

For the neutral, the differences between the two conformations are less distinct. Results for both conformations with each of the six functionals studied are presented in Table 11. All functionals, except B3P86 and BP86, predict conformation A to be a minimum and to be more stable than B, though by less than 0.09 kcal/mol. Obviously, the CF_3 group is essentially a free rotor. Four functionals predict B to be a minimum, while BHLYP and LSDA predict B to be a transition state. The anomalous predictions of A as a transition state by both B3P86 and BP86, and the disagreement over whether B is a minimum or transition state is not surprising considering the very flat potential for the CF_3 rotation. Similar inconsistencies were encountered in studying the flat, Jahn−Teller distorted, pseudorotatory surface of the cylcopentadienyl radical (C_5H_5) by Rienstra-Kiracofe, Graham, and Schaefer.[13] In that study, results were improved by using a larger integration grid within the Gaussian 94 program.[29] While increasing the quality of the integration grid may likely clarify the results for conformations A and B, the small energy differences involved approach the accuracy limit of the current DFT functionals.

Nonetheless, because of the near uniform agreement that conformation A is lower than B, and in the two exceptions (B3P86 and BP86), the small magnitude of the imaginary frequencies we report here results only for conformation A, which is directly comparable to the conformation studied for the anion. Furthermore, the small energy differences between A and B suggest that no matter which conformation is the true minimum, the overall electron affinity prediction for TFAE will not be significantly affected.

Results of geometry optimizations and harmonic frequency predictions for conformation A are given in Tables 12 and 13 Table XXIII (Supporting Information), respectively. The geometry of the neutral is not considerably different from that of the anion. With an additional electron, the H_2C-CO distance ($r3$) decreases by about 0.04 Å and the C−O distance (r_4) increases by about 0.03 Å.

Our electron affinity predictions for TFAE are very good for three functionals: the B3LYP result nearly matches the experimental value, and both BLYP and BP86 are within 0.1 eV. The B3P86, BHLYP, and LSDA functionals are all significantly in error. ZPVE-corrected EAs are at most only slightly lower by 0.01 eV.

E. C_4O. C_4O is a member of the important C_nO cluster family which are likely interstellar molecules.[105] Triplet linear C_4O was observed by Van Zee, Smith, and Weltner via electron spin resonance (ESR) in neon and argon matrices in 1988.[106] Their results suggested that C_4O is a $^3\Sigma^-$ state with cumulene-like bonding. That same year Maier, Reisenauer, Schäfer, and Balli observed the same ESR signal and also measured the IR absorption spectrum.[107] Later Ohshima, Endo, and Ogata investigated C_4O via microwave spectroscopy and observed spectra consistent with a $^3\Sigma$ state.[108] The electron affinity of C_4O was determined by Oakes and Ellison in 1986 via photoelectron spectroscopy to be 2.05 ± 0.15 eV.[109]

Our theoretical predictions also support a linear $^3\Sigma^-$ cumulene-like structure and are given in Table 14. Geometric parameters for C_4O and its anion are shown in Figure 7. The cumulene-like structure is suggested by the similar C−C bond distances. Other theoretical results have been reported,[110−112] and of particular interest are the results of Moazzen-Ahmadi and Zerbetto[112] at the BLYP/6-311G* level of theory, which gives bond lengths of 1.320, 1.294, 1.291, and 1.1796 for r_1, r_2, r_3, and r_4, respectively. Our BLYP predicted lengths are slightly longer, most likely due to the added diffuse functions in our DZP++ basis set. The anion geometries suggest that the additional electron partially removes the cumulene nature of the neutral molecule in favor of two separated carbon double bonds and also elongates the C−O bond. Indeed, the anion SOMO is a π MO that is bonding between the p orbitals on C_4 and C_3 (r_1) and between C_2 and C_1 (r_3), and antibonding between C_3 and C_2 (r_2) and between C1 and O (r_4).

Our harmonic vibrational frequencies for both the neutral and anion are given in Table 15 and Table XXIV (Supporting Information). We have compared our neutral frequency predictions to the experimental results of Maier et al.[107] We find excellent agreement and can rank the functionals according to mean absolute percent deviation from experiment: B3LYP (1.7%), B3P86 (2.0%), LSDA (2.1%), BP86 (3.6%), BLYP (4.4%), BHLYP (6.3%). As usual, BHLYP predicts frequencies highest in magnitude. While the data set is too small to draw any conclusions about the individual functionals, the close agreement with experiment is reassuring.

Because the anion ground state is a $^2\Pi$ state, C_4O^- it can be expected to exhibit Renner−Teller splitting in each of the Π bending normal modes. Analysis of the harmonic vibrational frequencies reveals that C_4O^- is a Renner−Teller case A molecule[113] with respect to each Π normal mode for all six functionals. This suggests that the anion will remain at a linear geometry. Indeed, Kannari, Aoki, Hashimoto, and Ikuta investigated a bent "V"-like structure for C_4O^- and found it to be higher in energy than the linear structure.[111] It is interesting to note that while all six functionals predict a larger frequency for the "in plane" bending mode than the "out of plane" bending mode for ω_5 and ω_7, only three functionals predict the larger frequency to be "in plane" for ω_6. This effect is likely because the splitting in ω_6 is small.

TABLE 11: Summary of the Performance of Six Functionals in Predicting the Relative Energies (in kcal/mol) of Two Conformations of 1,1,1-Trifluoroacetone Enolate Radical[a]

	B3LYP		B3P86		BHLYP		BLYP		BP86		LSDA	
	A	B	A	B	A	B	A	B	A	B	A	B
rel energy	0.0	0.025	0.0	−0.058	0.0	0.075	0.0	0.0077	0.0	−0.092	0.0	0.086
min or TS	min	min	TS (0.6i)	min	min	TS (−5i)	min	min	TS (11i)	min	min	TS (12i)

[a] Conformation A is shown in Figure 6, and conformation B is similar to A, except that the CF_3 group has been rotated 180°. Both conformations display C_s symmetry.

TABLE 12: Optimized Geometries for 1,1,1-Trifluoroacetone Enolate and Its Anion (C_s Symmetry)[a]

	B3LYP		B3P86		BHLYP		BLYP		BP86		LSDA	
	neut	anion	neut	anion	neut	anion	neut	anion	neut	anion	neut	anion
r_1	1.087	1.089	1.087	1.088	1.079	1.081	1.095	1.097	1.096	1.098	1.097	1.097
r_2	1.086	1.086	1.085	1.085	1.077	1.077	1.093	1.093	1.094	1.095	1.096	1.095
r_3	1.427	1.384	1.424	1.380	1.414	1.370	1.437	1.397	1.436	1.395	1.416	1.381
r_4	1.241	1.272	1.236	1.268	1.230	1.259	1.254	1.286	1.250	1.282	1.240	1.270
r_5	1.557	1.556	1.550	1.547	1.539	1.542	1.574	1.570	1.567	1.562	1.539	1.530
r_6	1.345	1.367	1.338	1.360	1.326	1.345	1.364	1.390	1.357	1.382	1.334	1.356
r_7	1.354	1.372	1.347	1.365	1.334	1.349	1.376	1.398	1.368	1.389	1.345	1.362
θ_1	120.2	119.1	120.3	119.2	120.3	119.2	120.1	119.0	120.2	119.1	120.7	119.7
θ_2	123.8	131.1	123.8	131.2	123.6	131.2	123.9	131.0	123.9	131.2	124.3	131.5
θ_3	118.9	115.8	118.8	115.7	119.3	115.9	118.7	115.8	118.6	115.7	118.3	115.4
θ_4	110.4	112.1	110.3	112.0	110.5	111.9	110.4	112.3	110.3	112.2	110.2	112.0
θ_5	112.2	116.2	112.2	116.1	111.9	115.8	112.5	116.6	112.5	116.6	112.0	116.0
θ_6	108.3	105.5	108.3	105.5	108.3	105.8	108.2	105.1	108.3	105.2	108.4	105.5

[a] Both the neutral ($^2A''$) and the anion ($^1A'$) geometries are given. (Bond lengths are in Å, and bond angles, in degrees.) Geometric parameters correspond to those shown in Figure 6.

TABLE 13: Harmonic Vibrational Frequencies ω_e (in cm^{-1}) for 1,1,1-Trifluoroacetone Enolate and Its Anion

		B3LYP		BLYP		BP86	
mode	symm	neut	anion	neut	anion	neut	anion
ω_1	A′	3297	3246	3211	3160	3218	3167
ω_2	A′	3175	3148	3093	3064	3096	3069
ω_3	A′	1544	1645	1486	1578	1522	1603
ω_4	A′	1469	1453	1426	1404	1420	1396
ω_5	A′	1355	1311	1283	1231	1298	1252
ω_6	A′	1182	1152	1096	1080	1122	1098
ω_7	A′	1147	1101	1088	1014	1105	1035
ω_8	A′	1016	1018	983	967	979	974
ω_9	A′	766	744	722	693	735	709
ω_{10}	A′	614	619	588	589	592	594
ω_{11}	A′	559	551	530	516	534	523
ω_{12}	A′	418	410	397	388	399	391
ω_{13}	A′	366	373	351	353	351	358
ω_{14}	A′	246	256	235	242	234	243
ω_{15}	A″	1178	1080	1086	981	1117	1014
ω_{16}	A″	850	737	828	698	816	703
ω_{17}	A″	663	653	627	624	627	622
ω_{18}	A″	496	603	469	573	473	557
ω_{19}	A″	422	496	382	466	374	472
ω_{20}	A″	242	260	232	247	230	247
ω_{21}	A″	11	55	5	51	11i	53

Our predicted electron affinities for C40 are all considerably higher than the experimental result of 2.05 ± 15.[109] Zero point corrections have no effect on the results. The one other theoretical EA prediction for C_4O by Kannari et al.[111] of 2.77 eV also supports our results. Motivated by the present work, we plan to examine the electron affinity of C_4O at very high levels of theory using convergent quantum mechanical methods. Oakes and Ellison noted that their photoelectron spectrum was "essentially unanalyzable". It appears likely that the reported experimental result should be reexamined.

F. Overall Functional Performance. Analysis of the optimized geometries for the carbon chain molecules studied with the local DFT functionals shows trends similar to those observed in prior studies. For instance, the BHYLP functional tends to predict the shortest bond lengths while the BLYP tends to predict the longest, a tendency that was observed by Tschumper and Schaefer[14] and Rienstra-Kiracoffe et al.[13] There is excellent agreement between the neutral tetracyanoethylene structure determined with neutron diffraction[82] and with the BHLYP structure, whereas all of the other functionals overestimate the bond lengths. Tschumper and Schaefer noted that all of the functionals, save BHLYP, overestimated the bond lengths significantly for diatomic and triatomic molecules,[14] and this trend holds true for TCNE. There were two disappointing occurrences, namely the uncertainty in the perfect linearity of neutral C_6H and in the favored conformation of neutral TFAE. Although in both cases the effect on the determination of the AEA is insignificant, this is a problem that warrants further theoretical study. It is important to note that geometry of the neutral and anionic species did not differ significantly in any computations performed and therefore comparison of the AEA with the experimentally determined values is reasonable.

Comparison of harmonic vibrational frequencies predicted from DFT with reliable experimentally assigned fundamental vibrations (i.e., modes in which the experimental assignment is not a matter of speculation, or for which the error in the experiment is so high that an accurate determination was not possible) can be used to evaluate the various functionals performance in predicting modes for this set of molecules. Using the 51 vibrational modes in the present study that fit this description, a ranking of the functionals by total percent difference from experiment was possible: BP86 (3.96%), BLYP (4.35%), B3LYP (4.76%), LSDA (5.17%), B3P86 (5.52%), and BHLYP (8.40%). Just as in the work of Rienstra-Kiracofe et al., the BP86 functional performs extremely well in predicting vibrational frequencies, whereas the BHLYP performs quite poorly.[13] Scott and Radom determined that the scaling factors between DFT harmonic vibrational frequencies and fundamental experimental frequencies ranged from 0.9945 to 0.9573 from their calculations on a set of 1066 experimental frequencies.[114] They also showed that the pure Becke-based DFT functionals showed the scaling factors close to unity and could often be

TABLE 14: Optimized Geometries for C_4O and Its Negative Ion (Both $C_{\infty v}$ Symmetry)[a]

	B3LYP		B3P86		BHLYP		BLYP		BP86		LSDA	
	neut	anion	neut	anion	neut	anion	neut	anion	neut	anion	neut	anion
r_1	1.323	1.288	1.323	1.288	1.309	1.272	1.336	1.303	1.337	1.304	1.324	1.293
r_2	1.298	1.346	1.298	1.346	1.286	1.340	1.309	1.353	1.308	1.351	1.300	1.340
r_3	1.295	1.269	1.295	1.269	1.286	1.255	1.304	1.281	1.304	1.281	1.295	1.274
r_4	1.177	1.218	1.177	1.218	1.160	1.202	1.193	1.233	1.190	1.229	1.180	1.216

[a] Both the neutral ($^3\Sigma^-$) and anion ($^2\Pi$) geometries for each method are given. (Bond lengths are in Å, and bond angles, in degrees.) Geometric parameters correspond to those shown in Figure 7.

TABLE 15: Harmonic Vibrational Frequencies ω_e (in cm^{-1}) for C_4O and Its Anion

mode and symm		B3LYP		BLYP		BP86		expt
neut	anion	neut	anion	neut	anion	neut	anion	neut[a]
$\omega_1\,\Sigma$	$\omega_1\,\Sigma$	2287	2246	2198	2162	2224	2186	2221.7
$\omega_2\,\Sigma$	$\omega_2\,\Sigma$	1958	1918	1873	1837	1891	1852	1922.7
$\omega_3\,\Sigma$	$\omega_3\,\Sigma$	1446	1448	1382	1382	1390	1398	1431.5
$\omega_4\,\Sigma$	$\omega_4\,\Sigma$	763	743	732	715	737	721	774.8
$\omega_5\,\Pi$	$\omega_{5a}\,(\Pi)^b$	478	532	438	489	444	492	484.0
$\omega_5\,\Pi$	$\omega_{5b}\,(\Pi)^c$	478	444	438	415	444	420	484.0
$\omega_6\,\Pi$	$\omega_{6a}\,(\Pi)^b$	349	392.1	310	364	298	358	
$\omega_6\,\Pi$	$\omega_{6b}\,(\Pi)^c$	349	391.8	310	337	298	336	
$\omega_7\,\Pi$	$\omega_{7a}\,(\Pi)^b$	129	151	124	145	121	143	
$\omega_7\,\Pi$	$\omega_{7b}\,(\Pi)^c$	129	112	124	95	121	87	

[a] Matrix isolation IR: ref 107. [b] Bending is in plane with respect to the SOMO. [c] Bending is out of plane with respect to the SOMO.

TABLE 16: Adiabatic Electron Affinities (in eV) of the Molecules Studied[a]

molecule	B3LYP	B3P86	BHLYP	BLYP	BP86	LSDA	expt
C_6	4.00	4.57	3.89	3.78	4.01	4.68	4.185 ± 0.006^b
	(4.02)	(4.59)	(3.91)	(3.80)	(4.04)	(4.71)	
C_7	3.43	4.03	3.58	3.10	3.36	3.90	3.358 ± 0.014^b
	(3.39)	(3.99)	(3.52)	(3.07)	(3.33)	(3.88)	
C_8	4.18	4.76	4.10	3.93	4.18	4.83	4.379 ± 0.006^b
	(4.19)	(4.77)	(4.11)	(3.95)	(4.19)	(4.85)	
C_9	3.73	4.33	3.94	3.38	3.64	4.20	3.684 ± 0.010^b
	(3.70)	(4.31)	(3.88)	(3.35)	(3.62)	(4.18)	
C_6H	3.65	4.23	3.48	3.45	3.69	4.35	3.8054 ± 0.015^c
	(3.66)	(4.24)	(3.50)	(3.48)	(3.72)	(4.38)	
C_6N_4	3.51	4.10	3.46	3.28	3.51	4.08	3.17 ± 0.20^d
	(3.49)	(4.07)	(3.43)	(3.26)	(3.49)	(4.06)	
CF_3CHCHO	2.61	3.12	2.29	2.55	2.71	3.40	2.6525 ± 0.010^e
	(2.60)	(3.12)	(2.29)	(2.54)	(2.70)	(3.40)	
C_4O	2.97	3.52	2.83	2.79	2.99	3.61	2.05 ± 0.15^f
	(2.98)	(3.52)	(2.83)	(2.79)	(2.99)	(3.61)	

[a] The harmonic zero-point vibrational energy (ZPVE) corrected electron affinities are listed in parentheses. [b] Photoelectron spectroscopy: see ref 33. [c] Photoelection spectroscopy: see ref 68. [d] Ion/molecule reaction equilibria: See refs 97 and 98. [e] Ion cyclotron resonance spectroscopy: see ref 104. [f] Photoelectron spectroscopy: see ref 109.

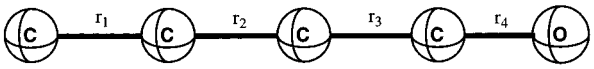

Figure 7. Geometric parameters for C_4O and its anion. Optimized geometries are given in Table 14.

used without scaling. It would appear that our results are consistent with this trend in that the two pure Becke-based functionals showed the closest agreement with experiment. It should be noted that this fortuitous agreement does not result from the functionals being more accurate, but from the fact that they tend to overestimate bond lengths at the equilibrium and therefore exhibit overall lowering in the calculated frequencies. In this case, since DFT tends to overestimate vibrational frequencies, it is to our advantage that this lowering occurs. The functionals, of course, are not actually reproducing anharmonic effects.

The main purpose of this study is the comparison of the AEA's predicted from the DFT functionals with known experimental values. Excluding the C_4O molecule, for which we suggest that the experimental determination is in error, the average absolute error for the various functionals and their ranking according to this parameter are as follows (in eV): BP86 (0.13), B3LYP (0.15), BLYP (0.28), BHLYP (0.29), B3P86 (0.56), LSDA (0.60). This ranking is consistent with the relative ranking of Rienstra-Kiracoffe et al.[13] and the average absolute errors show improvement over the accuracy of these methods on estimating the AEA of small molecules, as already seen in the determination of the AEA's of large ring molecules using DFT methods.[13] From examination of Tschumper and Schaefer's average absolute errors for the determination of the AEA's of atoms, diatomic, and triatomic molecules compared to experiment, we experience a 0.03−0.15 eV improvement in agreement. This is true for all functionals but the BLYP functional, which actually shows a 0.07 eV loss in agreement. The agreement reported by Rienstra-Kiracofe et al. is nearly the same as ours for all of the functionals besides BLYP, which shows a degradation in agreement of 0.08 eV, so it appears that the BLYP functional does not perform as well in the case of these molecules as it does for the small molecules and large rings.

The effect of ZPVE corrections to the AEA has been discussed in the individual results sections.

In addition to the above results, a collective set of 49 electron affinities predictions by each functional was examined by including 7 of the molecules presented in this work (C_4O was excluded), 8 of the medium ring compounds from Rienstra-Kiracoffe et al.,[13] and the previous results of Tschumper and Schaefer:[14] 7 of the 8 atoms (excluding Be), 12 diatomic molecules (including a revised electron affinity for BO[115]), and 15 triatomic molecules. The average absolute errors from experiment for this entire set are (in eV): BLYP (0.21), B3LYP (0.21), BP86 (0.22), BHLYP (0.32), B3P86 (0.62), LSDA (0.70). As shown in the previous work, the BLYP, B3LYP, and BP86 show excellent agreement with experiment, often within the experimental error. The LSDA functional shows relatively poor agreement, which is expected because LSDA is the functional that would suffer most from the local density approximation.

It appears that the DFT functionals can be used to predict the AEA's of carbon containing molecules to a relatively high level of accuracy. So what then does this say about using DFT methods on molecular anions? This question speaks to the debate mentioned earlier concerning positive occupied orbital eigenvalues for Kohn−Sham orbitals. Out of the 96 calculations performed in this study, only the BLYP and BP86 functionals applied to the anionic species of TFAE yielded positive eigenvalues. While this does not actually say that the self-interaction problem does not exist for these molecules, it does show that the density functionals, even the pure DFT functionals, are giving realistic results for most of the molecules studied. So either the self-interaction problem is insignificant or the error associated in the use of a finite basis set is providing a fortuitous cancelation of errors. Either way, the relative accuracy of the electron affinities estimated for the molecules studied here is impressive and demonstrates that this is a useful technique for comparison with experiment for unknown molecules of the same nature.

IV. Conclusions

The geometric parameters, harmonic vibrational frequencies, and AEA have been predicted for the neutral and anionic species of eight medium-sized carbon-containing molecules using six common DFT functionals, and these results have been compared to know experimental values. Optimized geometries for both the neutral and the anionic species were reasonable for all functionals employed. Minor inconsistencies occured in the determination of the geometries of neutral C_6H and TFAE, and further theoretical study is necessary. Harmonic vibrational frequencies show good agreement with available experimental fundamentals for both neutral and anionic species for all functionals save the BHLYP hybrid functional. The BP86 functional showed impressive agreement with reliable experimental electron affinities for the molecules studied. In most cases, this functional provided results within experimental error. The B3LYP and BLYP showed similarly impressive agreement with experimental electron affinities. We believe that these functionals provide sufficient reliability in the determination of electron affinities, and based on the values predicted for the C_4O molecule, it is suggested that the experimental determination of the electron affinity of C_4O was incorrect. As shown in our prior studies,[13,14] the BP86, BLYP, and B3LYP functionals all provide relatively accurate AEA's. So it appears that these functionals could be used to greatly benefit experimental chemists in searching for molecules for which the electron affinity is not known or is difficult to determine, while still providing a computationally tractable method for determining the AEA of larger molecular systems.

Acknowledgment. This work was funded by the U.S. National Science Foundation, Grant CHE-9527468. The authors would like to thank Gregory S. Tschumper, Dr. Wesley D. Allen, and Edward Valeev for their many helpful discussions.

References and Notes

(1) Kohn, W.; Becke, A. D.; Parr, R. G. *J. Phys. Chem.* **1996**, *100*, 12974.
(2) Galbraith, J. M.; Schaefer, H. F. *J. Chem. Phys.* **1996**, *105*, 862.
(3) Rösch, N.; Trickey, S. B. *J. Chem. Phys.* **1997**, *106*, 8941.
(4) Tschumper, G. S.; Fermann, J. T.; Schaefer, H. F. *J. Chem. Phys.* **1995**, *104*, 3676.
(5) Ziegler, T.; Gutsev, G. L. *J. Comput. Chem.* **1991**, *13*, 70.
(6) King, R. A.; Mastryukov, V. S.; Schaefer, H. F. *J. Chem. Phys.* **1996**, *105*, 6880.
(7) Van Huis, T. J.; Galbraith, J. M.; Schaefer, H. F. *Mol. Phys.* **1996**, *89*, 607.
(8) Chong, D. P.; Ng, C. Y. *J. Chem. Phys.* **1993**, *98*, 759.
(9) King, R. A.; Galbraith, J. M.; Schaefer, H. F. *J. Phys. Chem.* **1996**, *100*, 6061.
(10) Cole, L. A.; Perdew, J. P. *Phys. Rev. A* **1982**, *25*, 1265.
(11) Grafton, A. K.; Wheeler, R. A. *J. Phys. Chem.* **1997**, *101*, 7154.
(12) Boesch, S. E.; Grafton, A. K.; Wheeler, R. A. *J. Phys. Chem.* **1996**, *100*, 10083.
(13) Rienstra-Kiracofe, J. C.; Graham, D. E.; Schaefer, H. F. *Mol. Phys.* **1998**, *94*, 767.
(14) Tschumper, G. S.; Schaefer, H. F. *J. Chem. Phys.* **1997**, *107*, 2529.
(15) Curtiss, L. A.; Redfern, P. C.; Raghavarchari, K.; Pople, J. A. *J. Chem. Phys.* **1998**, *109*, 42.
(16) Lee, C.; Yang, W.; Parr, R. G. *Phys. Rev. B* **1998**, *37*, 785.
(17) Perdew, J. P. *Phys. Rev. B* **1986**, *33*, 8822.
(18) Perdew, J. P. *Phys. Rev. B* **1986**, *34*, 7406.
(19) Becke, A. D. *J. Chem. Phys.* **1993**, *98*, 5648.
(20) Becke, A. D. *J. Chem. Phys.* **1992**, *98*, 1372.
(21) Becke, A. D. *Phys. Rev. A* **1988**, *38*, 3098.
(22) Vosko, S. H.; Wilk, L.; Nusair, M. *Can. J. Phys.* **1980**, *58*, 1200.
(23) Hohenberg, P.; Kohn, W. *Phys. Rev. B* **1964**, *136*, 864.
(24) Kohn, W.; Sham, L. J. *Phys. Rev. A* **1965**, *140*, 1133.
(25) Slater, J. C. *Quantum Theory of Molecules and Solids: The Self-Consistent Field for Molecules and Solids*; McGraw-Hill: New York, 1974; Vol. IV.
(26) Huzinaga, S. *J. Chem. Phys.* **1965**, *42*, 1293.
(27) Dunning, T. H., Jr. *J. Chem. Phys.* **1970**, *53*, 2823.
(28) Lee, T. J.; Schaefer, H. F. *J. Chem. Phys.* **1985**, *83*, 1784.
(29) Frisch, M. J.; Trucks, G. W.; Schlegel, H. B.; Gill, P. M. W.; Johnson, B. G.; Robb, M. A.; Cheeseman, J. R.; Keith, T.; Petersson, G. A.; Montgomery, J. A.; Raghavachari, K.; Al-Laham, M. A.; Zakrzewski, V. G.; Ortiz, J. V.; Foresman, J. B.; Cioslowski, J.; Stefanov, B. B.; Nanayakkara, A.; Challacombe, M.; Peng, C. Y.; Ayala, P. Y.; Chen, W.; Wong, M. W.; Andres, J. L.; Replogle, E. S.; Gomperts, R.; Martin, R. L.; Fox, D. J.; Binkley, J. S.; Defrees, D. J.; Baker, J.; Stewart, J. P.; Head-Gordon, M.; Gonzalez, C.; Pople, J. A. GAUSSIAN 94, (Revision C.3); Gaussian, Inc.: Pittsburgh, PA, 1995.
(30) Maier, J. P. *J. Phys. Chem.* **1998**, *102*, 3462.
(31) Kohno, M.; Suzuki, S.; Shiromaru, H.; Moriwaki, T.; Achiba, Y. *Chem. Phys. Lett.* **1998**, *282*, 330.
(32) Arnold, D. W.; Bradforth, S. E.; Kitsopoulos, T. N.; Neumark, D. M. *J. Chem. Phys.* **1991**, *95*, 8753.
(33) Arnold, C. C.; Neumark, D. M. *Study of Small Carbon and Silicon Clusters Using Negative Ion Photodetachment Techniques*; JAI Press Inc.: Greenwich, CT, 1995.
(34) Yang, S.; Taylor, K. J.; Craycraft, M. J.; Conceicao, J.; Pettiette, C. L.; Cheshnovsky, O.; Smalley, R. E. *Chem. Phys. Lett.* **1988**, *144*, 431.
(35) Szczepanski, J.; Ekern, S.; Vala, M. *J. Phys. Chem.* **1997**, *101*, 1841.
(36) Ohara, M.; Shiromaru, H.; Achiba, Y. *J. Chem. Phys.* **1997**, *106*, 9992.
(37) Xu, C.; Burton, G. R.; Taylor, T. R.; Neumark, D. M. *J. Chem. Phys.* **1997**, *107*, 3428.
(38) Szczepanski, J.; Ekern, S.; Chapo, C.; Vala, M. *Chem. Phys.* **1996**, *211*, 359.
(39) Forney, D.; Fulara, J.; Freivogel, P.; Jakobi, M.; Lessen, D. *J. Chem. Phys. 103*, 48 (95).
(40) Szczepanski, J.; Auerbach, E.; Vala, M. *J. Phys. Chem.* **1997**, *101*, 9296.
(41) Liu, R.; Zhou, X. *J. Chem. Phys.* **1993**, *99*, 1440.

(42) Arnold, C. C.; Zhoa, Y.; Kitsopoulos, T. N.; Neumark, D. M. *J. Chem. Phys.* **1992**, *97*, 6121.
(43) Heath, J. R.; Saykally, R. J. *J. Chem. Phys.* **1991**, *94*, 1724.
(44) Kranze, R. H.; Rittby, C. M. L.; Graham, W. *J. Chem. Phys.* **1996**, *105*, 5313.
(45) Kranze, R. H.; Withey, P. A.; Rittby, C. M. L.; Graham, W. R. M. *J. Chem. Phys.* **1995**, *103*, 6841.
(46) Orden, A. V.; Provencal, R. A.; Keutsch, F. N.; Saykally, R. J. *J. Chem. Phys.* **1996**, *105*, 6111.
(47) Orden, A. V.; Saykally, R. J. *Chem. Rev.* **1998**, *98*, 2313.
(48) Raghavachari, K. *J. Chem. Phys.* **1987**, *87*, 2191.
(49) Watts, J. D.; Bartlett, R. J. *J. Chem. Phys.* **1992**, *97*, 3445.
(50) Ohno, M.; Zakrzewski, V. G.; Ortiz, J. V.; von Niessen, W. *J. Chem. Phys.* **1997**, *106*, 3258.
(51) Martin, J. M. L.; Taylor, P. R. *J. Phys. Chem.* **1996**, *100*, 6047.
(52) Adamowicz, L. *J. Chem. Phys.* **1991**, *94*, 1241.
(53) Martin, J. M. L.; El-Yazal, J.; Francois, J.-P. *Chem. Phys. Lett.* **1996**, *252*, 9.
(54) Martin, J. M. L.; El-Yazal, J.; Francois, J.-P. *Chem. Phys. Lett.* **1995**, *242*, 570.
(55) Ortiz, J. V.; Zakrzewski, V. G. *J. Chem. Phys.* **1994**, *100*, 6614.
(56) Adamowicz, L. *Chem. Phys. Lett.* **1991**, *182*, 45.
(57) Schmatz, S.; Botschwina, P. *Chem. Phys. Lett.* **1995**, *245*, 136.
(58) Pless, V.; Suter, H. U.; Engels, B. *J. Chem. Phys.* **1994**, *101*, 4042.
(59) Wu, Z. J.; Meng, Q. B.; Zhang, S. Y. *Chem. Phys. Lett.* **1997**, *267*, 271.
(60) Martin, J. M. L.; Taylor, P. R. *Chem. Phys. Lett.* **1995**, *240*, 521.
(61) Guelin, M.; Green, S.; Thaddeus, P. *Astron. Astrophys.* **1987**, *175*, L5.
(62) Natterer, J.; Koch, W.; Schröder, D.; Goldberg, N.; Schwarz, H. *Chem. Phys. Lett.* **1994**, *229*, 429.
(63) Liu, R.; Zhou, X.; Pulay, P. *J. Chem. Phys.* **1992**, *97*, 1602.
(64) Sobolewski, A. L.; Adamowicz, L. *J. Chem. Phys.* **1995**, *102*, 394.
(65) Fehér, M.; Maier, J. P. *Chem. Phys. Lett.* **1994**, *227*, 371.
(66) Pauzat, F.; Ellinger, Y.; McLean, A. D. *Astrophys. J.* **1991**, *369*, L13.
(67) Woon, D. E. *Chem. Phys. Lett.* **1995**, *244*, 45.
(68) Taylor, T. A.; Xu, C.; Neumark, D. M. *J. Chem. Phys.* **1998**, *108*, 10018.
(69) Doyle, T. J.; Shen, L. N.; Rittby, C. M. L.; Graham, W. R. M. *J .Chem. Phys.* **1991**, *95*, 6224.
(70) Sustmann, R.; Dern, M.; Kasten, R.; Sicking, W. *Chem. Ber.* **1987**, *120*, 1315.
(71) Basilevsky, M. V.; Weinberg, N. N.; Zhulin, V. M. *Croat. Chem. Acta* **1984**, *57*, 1423.
(72) Fatiadi, A. J. *Synthesis* **1986**, *249*.
(73) Fatiadi, A. J. *Synthesis* **1987**, 959.
(74) Zheludev, A.; Grand, A.; Ressouche, E.; Schweizer, J.; Morin, B. G.; Epstein, A. J.; Dixon, D. A.; Miller, J. S. *Angew. Chem., Int. Ed. Engl.* **1994**, *33*, 1397.
(75) Kahn, S. D.; Pau, C. F.; Hehre, W. J. *Int. J. Quantum Chem., Quantum Chem. Symp.* **1988**, *22*, 575.
(76) Cioslowski, J.; Mixon, S. T.; Edwards, W. D. *J. Am. Chem. Soc.* **1991**, *113*, 1083.
(77) Cioslowski, J.; Mixon, S. T. *J. Am. Chem. Soc.* **1991**, *113*, 4142.
(78) Juanós Timoneda, J.; Peters, K. S. *J. Phys. Chem.* **1996**, *100*, 16864.
(79) Watanabe, Y.; Kashiwagi, H. *Int. J. Quantum Chem.* **1983**, *23*, 1739.
(80) Emery, L. C.; Edwards, W. D. *Int. J. Quantum Chem., Quantum Chem. Symp.* **1991**, *25*, 347.
(81) Cioslowski, J. *Int. J. Quantum Chem.* **1994**, *49*, 463.
(82) Becker, P.; Coppens, P.; Ross, F. K. *J. Am. Chem. Soc.* **1973**, *95*, 7604.
(83) Hope, H. *Acta Chem. Scand.* **1968**, *22*, 1057.
(84) Dixon, D. A.; Miller, J. S. *J. Am. Chem. Soc.* **1987**, *109*, 3656.
(85) Hinkel, J. J.; Devlin, J. P. *J. Chem. Phys.* **1973**, *58*, 4750.
(86) Miller, F. A.; Sala, O.; Devlin, P.; Overend, J.; Lippert, E.; Lüder, W.; Moser, H.; Varchmin, J. *Spectrochim. Acta* **1964**, *20*, 1233.
(87) Michaelian, K. H.; Rieckhoff, K. E.; Voigt, E. M. *Spectrosc. Lett.* **1977**, *10*, 99.
(88) Michaelian, K. H.; Rieckhoff, K. E.; Voigt, E. M. *J. Mol. Struct.* **1982**, *95*, 1.
(89) Takenaka, T.; Hayashi, S. *Bull. Chem. Soc. Jpn.* **1964**, *37*, 1216.
(90) Moszyńska, B. *Acta Phys. Pol.* **1968**, *33*, 959.
(91) Heim, P.; Dörr, F. *Ber. Bunsen-Ges. Phys. Chem.* **1965**, *69*, 453.
(92) Farragher, A. L.; Page, F. M. *Trans. Faraday Soc.* **1967**, *63*, 2369.
(93) Lyons, L. E.; Palmer, L. D. *Chem. Phys. Lett.* **1973**, *21*, 442.
(94) Chen, E. C. M.; Wentworth, W. E. *J. Chem. Phys.* **1975**, *63*, 3183.
(95) Lyons, L. E.; Palmer, L. D. *Aust. J. Chem.* **1976**, *29*, 1919.
(96) Mischanchuk, B. G.; Nazarenko, V. A. *Teor. Eksp. Khim.* **1977**, *13*, 423.
(97) Chowdhury, S.; Kebarle, P. *J. Am. Chem. Soc.* **1986**, *108*, 5453.
(98) Chowdhury, S.; Kebarle, P. *J. Am. Chem. Soc.* **1987**, *109*, 1286.
(99) Younkin, J. M.; Smith, L. J.; Compton, R. N. *Theor. Chim. Acta* **1976**, *41*, 157.
(100) Dewar, M. J. S.; Rzepa, H. S. *J. Am. Chem. Soc.* **1978**, *100*, 784.
(101) Tanner, D. D.; Deonarian, N.; Kharrat, A. *Can. J. Chem.* **1989**, *67*, 171.
(102) Hilal, S. H.; Carreira, L. A.; Karickhoff, S. W.; Melton, C. M. *Quantum Struct.-Act. Relat.* **1993**, *12*, 389.
(103) Zimmerman, A. H.; Reed, K. J.; Brauman, J. I. *J. Am. Chem. Soc.* **1977**, *99*, 7203.
(104) Brinkman, E. A.; Berger, S.; Marks, J.; Brauman, J. I. *J. Chem. Phys.* **1993**, *99*, 7586.
(105) Adams, N. G.; Smith, D.; Giles, K.; Herbst, E. *Astron. Astrophys.* **1989**, *220*, 269.
(106) Van Zee, R. J.; Smith, G. R.; Weltner, W., Jr. *J. Am. Chem. Soc.* **1988**, *110*, 609.
(107) Maier, G. H.; Reisenauer, P.; Schäfer, U.; Balli, H. *Angew. Chem., Int. Ed. Engl.* **1988**, *27*, 566.
(108) Ohshima, Y.; Endo, Y.; Ogata, T. *J. Chem. Phys.* **1995**, *102*, 1493.
(109) Oakes, J. M.; Ellison, G. B. *Tetrahedron* **1986**, *42*, 6263.
(110) Ewing, D. W. *J. Am. Chem. Soc.* **1989**, *111*, 8809.
(111) Kannari, H.; Aoki, K.; Hashimoto, K.; Ikuta, S. *Chem. Phys. Lett.* **1994**, *222*, 313.
(112) Moazzen-Ahmadi, N.; Zerbetto, F. *J. Chem. Phys.* **1995**, *103*, 6343.
(113) Lee, T. J.; Fox, D. J.; Schaefer, H. F.; Pitzer, R. M. *J. Chem. Phys.* **1984**, *81*, 356.
(114) Scott, A. P.; Radom, L. *J. Phys. Chem.* **1996**, *100*, 16502.
(115) Wenthold, G.; Kim, J. B.; Jonas, K. L.; Lineberger, W. C. *J. Phys. Chem.* **1997**, *101*, 4472.